CHEMISTRY
A European Journal

A Journal of ChemPubSoc Europe

Accepted Article

Title: Non-classical S-Heteroacenes with o-quinoidal conjugation and open-shell diradical character

Authors: Xueliang Shi, Tullimilli Y. Gopalakrishna, Qing Wang, and Chunyan Chi

To be cited as: *Chem. Eur. J.* 10.1002/chem.201701813

Link to VoR: http://dx.doi.org/10.1002/chem.201701813

Supported by ACES

WILEY-VCH

Non-classical *S*-Heteroacenes with *o*-quinoidal conjugation and open-shell diradical character

Xueliang Shi, Tullimilli Y. Gopalakrishna, Qing Wang, and Chunyan Chi*[a]

Abstract: A series of non-classical *S*-heteroacenes were synthesized and they exhibited intriguing physical properties and chemical reactivity which are very different from the classical acenes. X-ray crystallographic analyses revealed that all the acenothiophene derivatives **Ph-AT-1** – **Ph-AT-3** had an *o*-quinoidal π-conjugation with large bond length alternation, while the acenodithiophene derivative **Ph-ADT-3** easily dimerized or reacted with oxygen to form peroxy-bridged dimer. The long acenothiophene **Ph-AT-4** is also highly reactive. The origin of these unique properties was investigated carefully by both experiments and theoritical calculations. The high reactivity of the long non-classical *S*-heteroacenes can be explained by their intrinsic open-shell diradical character as well as the *o*-quinoidal conjugation.

Introduction

Acene-based molecules and materials have been the focus of research in the chemistry and materials communities due to their unique electronic properties and promising applications in organic electronics.[1] Modern theoretical and experimental studies suggest that acenes longer than hexacene possess an open-shell singlet ground state.[2] Similar to other quinoidal polycyclic hydrocarbons based open-shell singlet diradicaloids such as bisphenalenyls, zethrenes and indenofluorenes,[3] the appearance of the open-shell diradical or even polyradical character in long acenes is due to the diminished energy gap and recovery of one or more aromatic sextet rings in the diradical/polyradical form.[4] So far, while the electronic structures and physical properties of acenes have been well investigated, there are another type of non-classical *S*-heteroacene molecules such as acenothiophene (**AT-n**) and acenodithiophene (**ADT-n**) deserved deep studies but they are not well developed mainly due to synthetic challenges (Figure 1). Unlike traditional acenes, **AT-n** family can only be drawn in an *o*-quinoidal conjugation (diene conjugation) in the closed-shell resonance form if the hypervalent sulfur contribution is ignored (Figure 1), indicating a different electronic structure and higher reactivity compared with their corresponding acene analogues. In fact, the oligomers and polymers of **AT-1** (isothianaphthene) and **AT-2** (isonaphthothiophene) showed very small band gaps and can be easily doped into conducting polymers.[5]

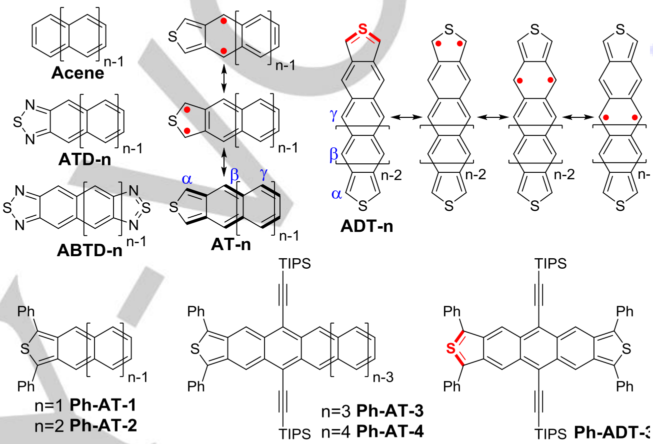

Figure 1. Structures of acene, acenothiophene (**AT-n**), acenodithiophene (**ADT-n**), acenothiadiazole (**ATD-n**), acenobisthiadiazole (**ABTD-n**), and the target molecules in this work. TIPS: triisopropylsilyl; Ph: phenyl.

Another class of non-classical *S*-heteroacenes, the acenodithiophene, has a peculiar non-Kekulé electronic structure with tetra-covalent sulfur as part of a thiophene ring (Figure 1). Thus **ADT-n** is also expected to exhibit distinctively different properties from its two isomers and normal acenes.[6] However, the early investigations were only limited to the **ADT-0** (thieno[3,4-*c*]thiophene) and **ADT-1** (thieno[3,4-*f*]isothianaphthene) derivatives which are already quite reactive and the longer homologs have never been successfully synthesized.[7] A similar system to non-classical *S*-heteroacenes are the acenothiadiazole (**ATD-n**) and acenobisthiadiazole (**ABTD-n**),[8] which are expected to possess higher stability because hypervalent sulfur (-N=S=N-) would participate in sulfur-nitrogen conjugation. Indeed, the shortest molecules **ATD-1** (benzothiadiazole) and **ABTD-1** (bisbenzothiadiazole) exhibit high stability and they have been widely used as semiconducting materials. Compared with the corresponding acenodithiophenes (**ADT-0** and **ADT-1**), they are more stable because hypervalent sulfur contribution in sulfur-carbon conjugation is less than that in sulfur-nitrogen conjugation.[9] However, recent studies also demonstrated that the extended thiadiazole systems such as **ATD-4**, **ABTD-2** and **ABTD-3** all became extremely unstable and the isolation was not successful.[10] Fundamentally, all these four systems (AT,

---

[a] Dr. X. Shi, Dr. T. Y. Gopalakrishna, Q. Wang, Prof. C. Chi
Department of Chemistry
National University of Singapore
3 Science Drive 3, 117543, Singapore
E-mail: chmcc@nus.edu.sg

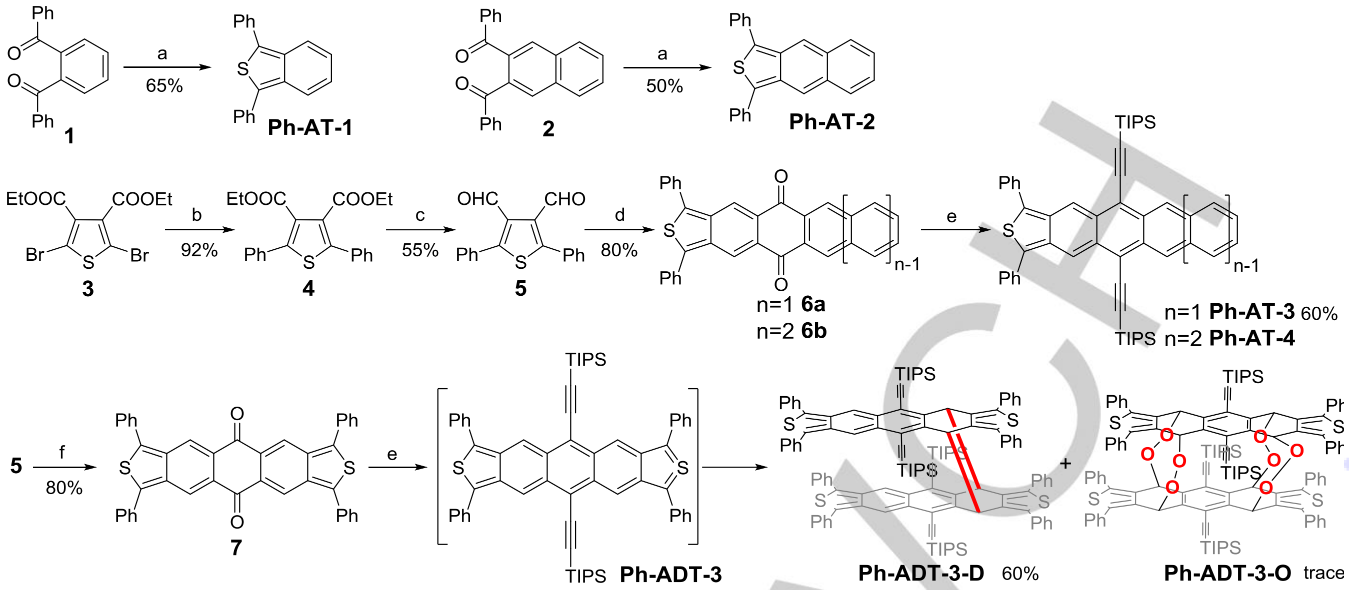

Scheme 1. *Reagents and conditions*: (a) Lawesson's reagent, toluene, reflux, overnight; (b) phenylboronic acid, $Pd(PPh_3)_4$, Na_2CO_3, toluene/water (4:1), 105 °C, 12h; (c) (i) $LiAlH_4$, dry THF, 0 °C – rt, overnight; (ii) PCC, DCM; (d) for **6a** 1,4-dihydroxynaphthalene, for **6b** 1,4-dihydroxyanthracene, 30% KOH (aq.), EtOH, 60 °C, overnight; (e) (i) TIPSCCLi, THF, 0 °C – rt, overnight; (ii) $SnCl_2$, 12 h; (f) 1,4-cyclohexanedione, 30% KOH (aq.), EtOH, 60 °C, overnight.

ADT, ATD, and ABTD) have the same number of π-electrons to the corresponding acene molecules, and thus they are the true isoelectronic structures of acenes. The origin of their high reactivity and unique properties are deserved further investigations. Recent insight to the diradical character of long acenes provoked us to re-consider the possible diradical character of these non-classical acenes.

Our spin-unrestricted DFT calculations (UCAM-B3LYP/6-31G(d,p)) indicate that long **AT-n** and **ADT-n** molecules indeed have an open-shell singlet ground state with appearance of diradical character (y_0 = 4.6%, 21.9%, 12.5%, 31.3%, 49.0% for **AT-3**, **AT-4**, **ADT-1**, **ADT-2**, and **ADT-3**, respectively), and the ADT family has a relatively larger diradical character and smaller singlet-triplet gap compared to AT family with the same number of fused rings (Table S1 in ESI†). Similar trend was observed in the ATD and ABTD family (y_0 = 1.4%, 14.9%, 0.6%, 14.9%, 35.3% for **ATD-3**, **ATD-4**, **ABTD-1**, **ABTD-2**, and **ABTD-3**, respectively), but they display smaller diradical character and larger singlet-triplet gap compared to the respective **AT**s and **ADT**s (Table S1 in ESI†). Simple resonance form analysis (Figure 1) indicates high spin densities at the zig-zag edges (α, β, γ sites), which is also supported by the calculated spin density distribution map (Figure S1 in ESI†). Therefore, proper blocking groups such as phenyl and triisopropylsilyl ethynyl should be attached to these reactive sites to obtain stable compounds. In this work, the synthesis, structure, physical property and chemical reactivity of several kinetically blocked **AT**s and **ADT**s (Figure 1) will be reported and discussed, which provide important insights to the intrinsic properties of these non-classical acene molecules.

Results and Discussion

Synthesis and structural characterization

The phenyl-substituted shorter AT compound **Ph-AT-1** and **Ph-AT-2** were synthesized from diketones **1** and **2**, respectively, by a modified procedure from literatures.[11] The synthesis of longer **AT-n** and **ADT-n** derivatives are based on the corresponding quinones (Scheme 1). Suzuki coupling reaction between 2,5-dibromo-3,4-diethylcarboxylthiophene **3**[12] and phenyl boronic acid gave the diester **4**, which was converted into the dialdehyde **5** by reduction with lithium aluminium hydride ($LiAlH_4$) followed by oxidation of the intermediate diol with pyridinium chlorochromate (PCC). The quinones **6a-b** and **7** were then obtained from the condensation reaction between **5** and 1,4-dihydroxynaphthalene**,** 1,4-dihydroxyanthracene and 1,4-cyclohexanedione, respectively. Addition of triisopropylsilyl ethynyl lithium to the quinone **6a** and reduction of the intermediate diol by $SnCl_2$ gave **Ph-AT-3** as a deep green solid. Following the same protocol, **Ph-AT-4** and **Ph-ADT-3** turned out to be extremely reactive although they are well kinetically blocked. For **Ph-AT-4**, MALDI-TOF mass spectrum of the reaction solution showed obvious peaks for the oxygen-addition products (Figure S6 in ESI†) but the isolation of the products was not successful due to the quick decomposition into complicated mixtures during the workup. Interestingly, **Ph-ADT-3** quickly dimerized to form a covalently linked dimer **Ph-ADT-3-D** which was confirmed through X-ray crystallographic analysis (Figure 2a). In addition, during the crystal growing of **Ph-ADT-3-D**, a trace amount of peroxy-linked dimer **Ph-ADT-3-O** was also occasionally identified by X-ray crystallographic analysis (Figure 2a).

Single crystals suitable for crystallographic analysis were obtained for **Ph-AT-1** – **Ph-AT-3** and the two dimers **Ph-ADT-3-D** and **Ph-ADT-3-O** (Figure 2a).[13] **Ph-AT-1** – **Ph-AT-3** all have a planar backbone and bond length analysis of the backbone clearly revealed an *o*-quinoidal conjugation motif with large bond length alternation (Figure 2b). The dimerization of the **Ph-ADT-3** happened between the four unblocked carbon centers along the zig-zag edges in the *cis*- mode. Although the quality of **Ph-ADT-3-O** crystals was not good enough for bond length analysis, its chemical structure could be confirmed clearly. It is a peroxy-bridged dimer with four peroxy groups linked to the all unblocked sites. No close π-π stacking was observed for all these molecules due to the attached bulky groups.

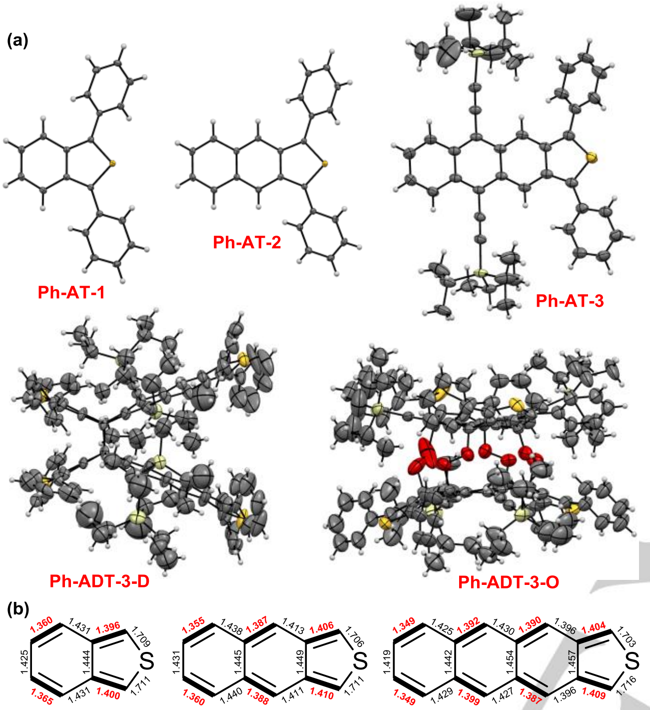

Figure 2. (a) X-ray crystallographic structures of **Ph-AT-1**, **Ph-AT-2**, **Ph-AT-3**, **Ph-ADT-3-D** and **Ph-ADT-3-O**. (b) Selected bond lengths of the backbones of **Ph-AT-1**, **Ph-AT-2** and **Ph-AT-3** showing *o*-quinoidal conjugation.

DFT calculations

Same level calculations predicted that the **Ph-AT-1** and **Ph-AT-2** both would have a closed-shell ground state (Table S1 and Figure S1 in ESI†), but the **Ph-AT-3**, **Ph-AT-4** and **Ph-ADT-3** all have an open-shell singlet ground state with significant diradical characters (y_0 = 8.9%, 27.9%, 54.2% for **Ph-AT-3**, **Ph-AT-4** and **Ph-ADT-3**, respectively). The singly occupied molecular orbital (SOMO) profiles of the α and β spins and the spin density distribution of **Ph-AT-3**, **Ph-AT-4** and **Ph-ADT-3** in the open-shell singlet state are shown in Figure 3 and all of them display a disjoint character, and accordingly, the spin densities (spin α – spin β) are mainly distributed along the two zig-zag edges. The larger the SOMO-α and SOMO-β orbital segregation, the larger the diradical character. The moderate diradical characters explain their high reactivity and it seems that kinetical blocking of all α, β and γ carbons is necessary to obtain stable compounds; otherwise, intermolecular dimerization or reaction with oxygen will happen. It was also noted that although **Ph-AT-3** was predicted to have an open-shell singlet ground state, experimentally, sharp NMR spectrum was observed and there is no ESR signal, which can be explained by its relatively large singlet-triplet gap (12.8 kcal/mol based on calculation). Anisotropy of the induced current density (ACID) plots of all these non-classical *S*-heteroacenes clearly revealed a clockwise diatropic ring current delocalized along the peripheries of the π-conjugated framework (Figure 4), indicating their aromatic character similar to the corresponding acenes, which is reasonable considering that they possess the same number of delocalized [4*n*+2] π electrons. However, they have distinctively different electronic structures and thus display different chemical reactivity.

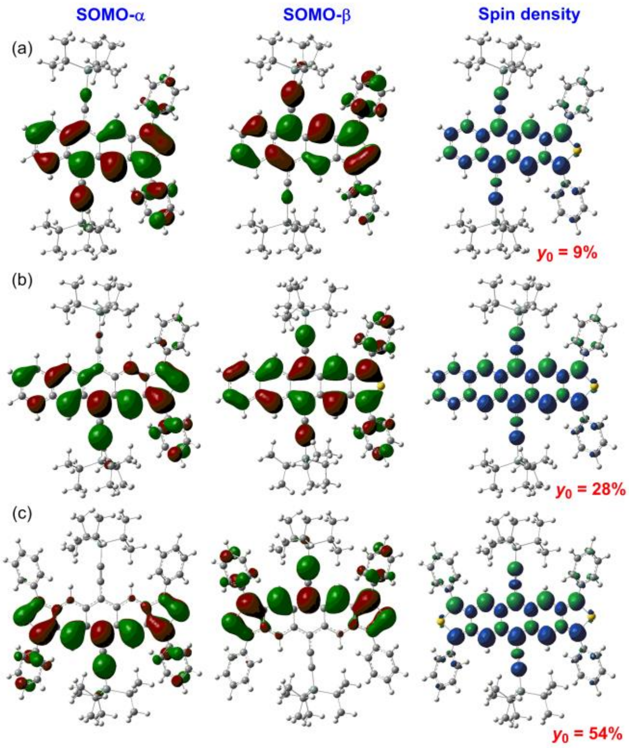

Figure 3. Calculated frontier SOMO-α/β profiles and spin density distribution of **Ph-AT-3** (a), **Ph-AT-4** (b) and **Ph-ADT-3** (c); y_0: diradical character index.

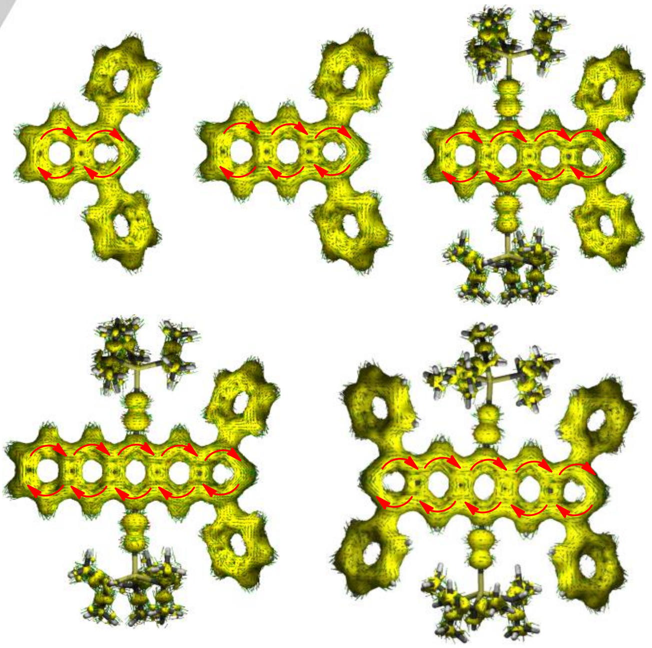

Figure 4. Calculated ACID curves of **Ph-AT-n** (n = 1-4) and **Ph-ADT-3**. The red arrows indicate clockwise ring current pathway.

Table 1. Summary of the optical and electrochemical data of **Ph-AT-1**, **Ph-AT-2**, **Ph-AT-3** and **Ph-ADT-3-D**

Compound	λ_{max} (nm)[a]	$E_{1/2}^{red}$ (V) [b]	$E_{1/2}^{ox}$ (V) [b]	E_{red}^{onset} (V) [c]	E_{ox}^{onset} (V) [c]	HOMO (eV) [d]	LUMO (eV) [d]	E_g^{EC} (eV) [e]	Eg^{opt} (eV)[f]
Ph-AT-1	269 395		0.56, 1.23		0.46	-5.26	-2.47[g]		2.79
Ph-AT-2	257, 290 513	-2.07	0.28, 1.04	-1.98	0.18	- 4.98	-2.82	2.16	2.21
Ph-AT-3	317 698	-1.53, -1.98	0.16, 0.82	-1.44	0.08	-4.88	-3.36	1.53	1.63
Ph-ADT-3-D	259 547	-1.98	0.30, 0.41	-1.87	0.18	-4.98	-2.93	2.05	2.06

[a] λ_{max} is the wavelength of absorption maximum; [b] $E_{1/2}^{red}$ and $E_{1/2}^{ox}$ are the half-wave potentials for respective oxidation and reduction waves with Fc/Fc^+ as reference. [c] E_{red}^{onset} and E_{ox}^{onset} are the onset potentials of the first reductive and oxidative redox wave with Fc/Fc^+ as reference, respectively. [d] HOMO and LUMO energy levels were calculated according to the equations HOMO = −(4.8 + E_{ox}^{onset}) and LUMO = −(4.8 +E_{red}^{onset}). [e] E_g^{Ec} is the electrochemical energy gap derived from LUMO−HOMO. [f] Eg^{opt} is the optical energy gap calculated from the low-energy absorption edge. [g] The LUMO energy level of **Ph-AT-1** was calculated according to the equation LUMO = Eg^{opt} + HOMO.

Optical and electrochemical properties

The UV-vis absorption data of **Ph-AT-1** – **Ph-AT-3** and the dimer **Ph-ADT-3-D** in dichloromethane (DCM) are shown in Figure 5a and Table 1. All the compounds characteristically display two major bands, one high-energy band with the peak around 300 nm, and another broad band at low-energy region, which essentially differs from the absorption spectra of functionalized acenes.[1b] The second band of **Ph-AT-1** – **Ph-AT-3** is red shifted with increase of the molecular length, with the absorption maximum (λ_{max}) at 395, 513 and 698 nm, respectively. The absorption spectrum of **Ph-ADT-3-D** is quite similar to that of **Ph-AT-2** because they have the same thieno[3,4-*f*]isothianaphthene chromophore. Compared with the absorption spectra of substituted **ATD-n**,[8a] the absorption spectra of **Ph-AT-1** – **Ph-AT-3** are entirely different and red-shifted about 100 nm although they have large structural similarity. Such difference can be explained by the larger diradical characters in the **AT** system.

The electrochemical properties of **Ph-AT-1** – **Ph-AT-3** and the dimer **Ph-ADT-3-D** were investigated by cyclic voltammetry in dry DCM solution (Figure 5b and Table 1). All compounds showed two (quasi-) reversible oxidation waves with half-wave potential $E_{1/2}^{ox}$ at 0.56, 1.23 V for **Ph-AT-1**, 0.28, 1.04 V for **Ph-AT-2**, 0.16, 0.82 V for **Ph-AT-3** and 0.30, 0.41 V for **Ph-ADT-3-D** (*vs* Fc^+/Fc). In the case of their reduction waves, **Ph-AT-2** and **Ph-ADT-3-D** exhibited one reduction wave at $E_{1/2}^{red}$ = -2.07 and -1.98 V, respectively, while **Ph-AT-3** displayed two reduction waves at $E_{1/2}^{red}$ = -1.98, -1.53 V. No reduction wave was found for **Ph-AT-1**. It is found that extension of the molecular size leads to a rising of the HOMO energy level (HOMO = -5.26, -4.98 and -4.88 eV for **Ph-AT-1**, **Ph-AT-2**, **Ph-AT-3**, respectively). The dimer **Ph-ADT-3-D** has the same HOMO energy level to **Ph-AT-2** but slightly lower LUMO energy level (-2.93 eV for **Ph-ADT-3-D**, LUMO = -2.82 eV for **Ph-AT-2**). The electrochemical energy gaps (E_g^{EC}) are well consistent with their optical energy gap (E_g^{opt}), which both decrease with the increase of their molecular length. Due to the electron-rich nature of this series of compounds, their radical cations were easily obtained by oxidation with $SbCl_5$ in DCM and characterized by UV-vis-NIR absorption spectra (Figure 6). Only the dication of the dimer **Ph-ADT-3-D** is achievable while dications of **Ph-AT-1** – **Ph-AT-3** is not accessible by oxidation with $SbCl_5$ due to the high second oxidation half-wave potentials.

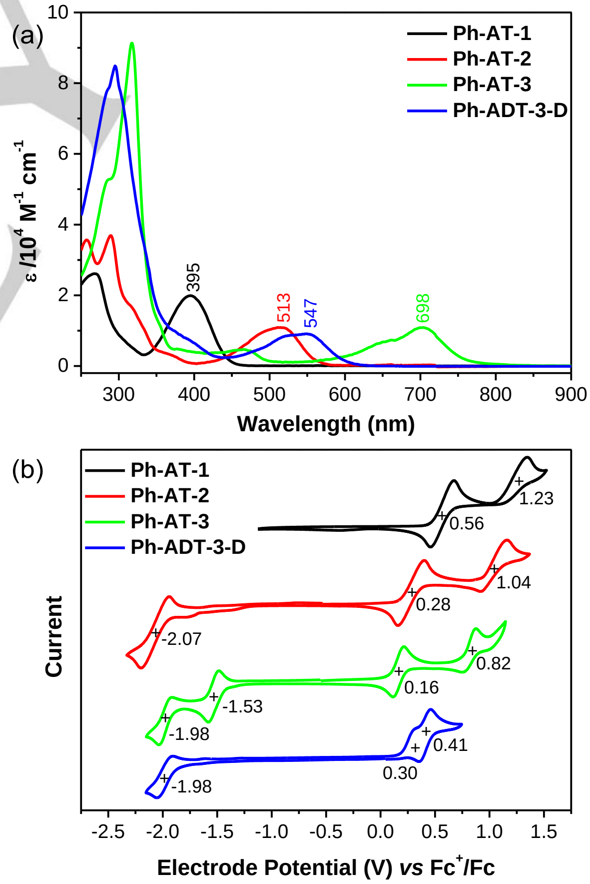

Figure 5. (a) UV-vis-NIR absorption spectra of **Ph-AT-1**, **Ph-AT-2**, **Ph-AT-3**, and **Ph-ADT-3-D** recorded in DCM. (b) Cyclic voltammograms of **Ph-AT-1**, **Ph-AT-2**, **Ph-AT-3**, and **Ph-ADT-3-D** in DCM with 0.1 M Bu_4NPF_6 as supporting electrolyte, Ag/AgCl as reference electrode, Pt wire as counter electrode, and scan rate at 50 mV/s. Fc: ferrocene. The electrode potential was externally calibrated by Fc^+/Fc couple.

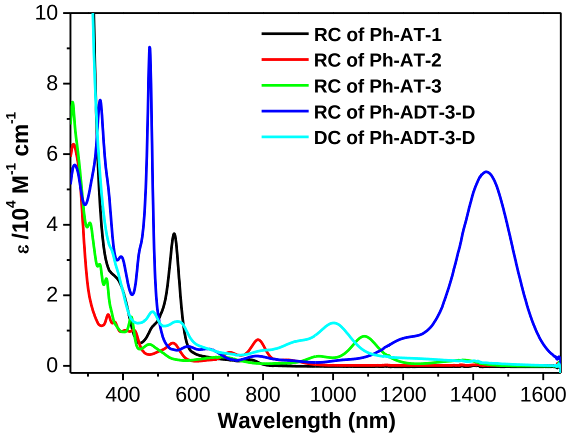

Figure 6. UV-vis-NIR absorption spectra of oxidized species of **Ph-AT-n** (n=1-3) and **Ph-ADT-3-D** by titration with $SbCl_5$ in dry DCM. RC: radical cation; DC: dication. The radical cations were obtained by using one equivalent $SbCl_5$, and dication of **Ph-ADT-3-D** was obtained by using two equivalent $SbCl_5$.

Photo-Stability test

Photo-stability tests of **Ph-AT-1** – **Ph-AT-3** and the dimer **Ph-ADT-3-D** in DCM solutions were conducted (1×10^{-5} M) under dark and ambient light conditions (Figure 7 and Figure S2 in ESI†). It was found that except the shortest molecule **Ph-AT-1** (half lifetime $t_{1/2}$ = 12 hours), such series of compounds are extraordinarily sensitive to light ($t_{1/2}$ = 5 min, 60 min and 10 min for **Ph-AT-2**, **Ph-AT-3** and **Ph-ADT-3-D**, respectively) and decompose quickly, but they are very stable and no obvious decomposition was found even within one week in ambient air condition without light! The high light sensitivity of these non-classical *S*-heteroacenes can be ascribed to their unique diene conjugation and increased diradical character with chain length, thus they are especially vulnerable to singlet oxygen under light irradiation. Their oxygen-addition products were detected by MALDI-TOF mass spectrometry (Fig. S3-5 in ESI†).

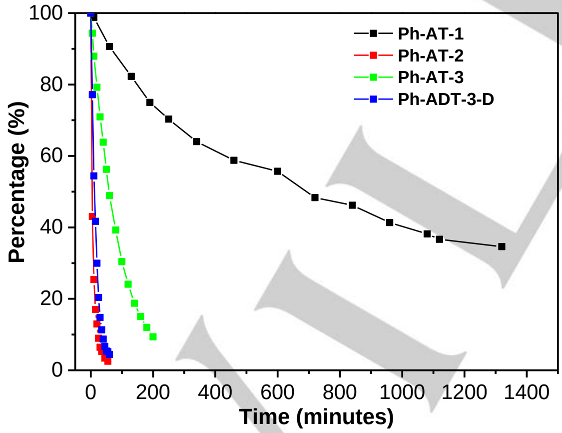

Figure 7. Changes of the optical density at long-wavelength absorption maximum (395 nm, 513 nm, 698 nm and 547 nm) with time for **Ph-AT-1**, **Ph-AT-2**, **Ph-AT-3** and **Ph-ADT-3-D** under ambient air and light conditions.

Conclusions

In summary, a series of kinetically blocked non-classical *S*-heteroacenes have been synthesized. Our detailed investigations on their geometric and electronic structures, optical and electrochemical properties, and chemical reactivity clearly revealed their very different behaviour from the classic acene molecules. X-ray crystallographic analyses revealed that all the acenothiophene derivatives **Ph-AT-1** – **Ph-AT-3** had an *o*-quinoidal conjugation with large bond length alternation, while the acenodithiophene derivative **Ph-ADT-3** easily dimerized or reacted with oxygen to form peroxy-bridged dimer. The long acenothiophene **Ph-AT-4** is also highly reactive. All these can be explained by their unique *o*-quinoidal conjugation and open-shell diradical character. Our studies give important insights to the intrinsic properties of the non-classical acenes, and our next-stage work is to synthesize very stable non-classical *S*-heteroacenes by using our recently developed stabilizing strategies for higher order acenes.[14]

Experimental Section

o-dibenzoyllbenzene **1**,[11a] naphthalene-2,3-dibis(phenylmethanone) **2**[11b] and 2,5-dibromo-3,4-diethylcarboxylthiophene **3**[12] were prepared according to the reported procedures.

General procedure for preparation of Ph-AT-1 and Ph-AT-2

To the solution of diketone **1** or **2** (1.0 mmol) in dry toluene (20 mL), Lawesson's reagent (2.0 mmol) was added and the reaction mixture was heated to reflux overnight under dark condition. After that removal of solvent directly followed by column chromatographic purification (silica gel, hexane, avoid light) gave **Ph-AT-1** (186 mg, 65%) and **Ph-AT-2** (168 mg, 50%) as a solid.

Ph-AT-1 Yellow solid, ^1H NMR (500 MHz, $CDCl_3$, ppm): δ = 7.85 (dd, *J* = 3.0, 6.9 Hz, 2H), 7.71 (d, *J* = 7.6 Hz, 4H), 7.51 (t, *J* = 7.6 Hz, 4H), 7.39 (t, *J* = 7.4 Hz, 2H), 7.11 (dd, J = 3.0, 6.9 Hz, 2H); ^{13}C NMR (125 MHz, $CDCl_3$, ppm): δ =135.17, 134.29, 134.15, 129.24, 129.00, 127.45, 124.19, 121.14; HRMS analysis (ESI): calcd for $C_{20}H_{14}S$ (M^+), 286.0811; found, 286.0813 (error: 0.7 ppm).

Ph-AT-2 Red solid, ^1H NMR (500 MHz, $CDCl_3$, ppm): δ = 8.43 (s 2H), 7.83 (d, *J* = 7.4 Hz, 4H), 7.70-7.65 (m, 2H), 7.57 (t, *J* = 7.7 Hz, 4H), 7.43 (t, *J* = 7.4 Hz, 2H), 7.17-7.12 (m, 2H); ^{13}C NMR (125 MHz, $CDCl_3$, ppm): δ =134.88, 134.72, 132.47, 131.43, 129.26, 129.18, 128.89, 127.34, 124.82, 118.45; HRMS analysis (ESI): calcd for $C_{24}H_{16}S$ (M^+), 336.0967; found, 336.0968 (error: 0.3 ppm).

Synthesis of 4

Phenylboronic acid (976 mg, 8.0 mmol), 2,5-dibromo-3,4-diethylcarboxylthiophene **3** (772 mg, 2.0 mmol), and Na_2CO_3 (848 mg, 8.0 mmol) were dissolved in water (6 mL) and toluene (30 mL). $Pd(PPh_3)_4$ (140 mg) was added as a catalyst and the mixture was refluxed for 12 h under argon. After cooling down cold methanol was added and a white precipitate was formed. The crude product **4** was collected by filtration and further purified by column chromatography (silica gel, hexane/DCM) as a white solid (700 mg, 92% yield). ^1H NMR (500 MHz, $CDCl_3$, ppm): δ = 7.54-7.48 (m, 4H), 7.43-7.38 (m, 6H), 4.22 (q, *J* = 8.9 Hz, 4H), 1.17 (t, *J* = 8.9 Hz, 6H); ^{13}C NMR (125 MHz, $CDCl_3$, ppm): δ =164.19, 145.69, 132.34, 130.11, 129.14, 128.85, 128.41, 61.34, 13.82; HRMS analysis (ESI): calcd for $C_{22}H_{20}O_4S$ (M + Na)$^+$, 403.0975; found, 403.0978 (error: 0.7 ppm).

Synthesis of 5

An ethereal solution of $LiAlH_4$ (379 mg, 10 mmol) in anhydrous THF (30 mL) was cooled to 0 °C and degassed *via* three freeze-thaw pump cycles. To the mixture, compound **4** (760 mg, 2.0 mmol) was added in small portions to avoid excessive gas evolution. The reaction mixture was stirred at 0 °C for 15 min, then allowed to warm to room temperature and stirred overnight. The mixture was acidified with 10% HCl solution, and then filtered to remove all solids. The filtered mixture was extracted with EtOAc, the organic layer was dried over anhydrous Na_2SO_4 and the solvent was removed by rotary evaporation to yield the diol as a waxy solid, which was used for the next step reaction without further purification and characterization. The above diol intermediate was dissolved in 40 mL of dichloromethane. PCC (1.30 g, 6.0 mmol) was slowly added into the solution by portions. The reaction was stirred overnight at room temperature and the resulting mixture was poured into water and extracted with dichloromethane. The combine extracts were dried over anhydrous Na_2SO_4, the solvent was removed in vacuum and the residue was purified by column chromatography (silica gel, hexane/DCM). The title compound **5** was obtained as faint yellow solid (321 mg, 55% yield for two steps). ^{1}H NMR (500 MHz, $CDCl_3$, ppm): δ = 10.21 (s, 2H), 7.59-7.54 (m, 4H), 7.52-7.47 (m, 6H); ^{13}C NMR (125 MHz, $CDCl_3$, ppm): δ = 187.33, 153.16, 135.47, 130.86, 130.09, 129.82, 128.76; HRMS analysis (ESI): calcd for $C_{18}H_{12}O_2S$ (M + Na)$^+$, 315.0450; found, 315.0455 (error: 1.6 ppm).

Synthesis of 6a

Dialdehyde **5** (584 mg, 2.0 mmol) and 1,4-dihydroxynaphthalene (320 mg, 2.0 mmol) were dissolved in EtOH (50 mL). An aqueous solution of 30% KOH (2 mL) was added and the mixture was stirred at 60 °C overnight. The resulting precipitate was filtered, washed with water, EtOH and hexane until the washings were colorless. The precipitate was further purified by column chromatography (silica gel, hexane/DCM), giving quinone **6a** as a yellow solid (666 mg, 80% yield). ^{1}H NMR (500 MHz, $CDCl_3$, ppm): δ = 8.83 (s, 2H), 8.36-8.32 (m, 2H), 7.78-7.74 (m, 2H), 7.72 (d, *J* = 8.0 Hz, 4H), 7.56 (t, *J* = 7.6 Hz, 4H), 7.48 (t, *J* = 7.4 Hz, 2H); ^{13}C NMR (125 MHz, $CDCl_3$, ppm): δ =182.76, 141.27, 134.89, 134.80, 133.91, 132.77, 129.43, 129.41, 128.74, 128.14, 127.43, 124.81; HRMS analysis (APCI): calcd for $C_{28}H_{16}O_2S$ (M+H)$^+$, 417.0944; found, 417.0948 (error: 1.0 ppm).

Synthesis of 6b

Dialdehyde **5** (584 mg, 2.0 mmol) and 1,4-dihydroxyanthracene (420 mg, 2.0 mmol) were dissolved in EtOH (50 mL). An aqueous solution of 30% KOH (2 mL) was added and the mixture was stirred at 60 °C overnight. The resulting precipitate was filtered, washed with water, EtOH and DCM until the washings were colorless, giving quinone **6b** as an insoluble brown solid (745 mg, 80% yield). HRMS analysis (APCI): calcd for $C_{32}H_{18}O_2S$ (M+H)$^+$, 467.1100; found, 467.1094 (error: -1.3 ppm).

Synthesis of 7

Dialdehyde **5** (584 mg, 2.0 mmol) and 1,4-cyclohexanedione (112 mg, 1.0 mmol) were dissolved in EtOH (50 mL). An aqueous solution of 30% KOH (2 mL) was added and the mixture was stirred at 60 °C overnight. The resulting precipitate was filtered, washed with water, EtOH and DCM until the washings were colorless, giving quinone **7** as an insoluble red solid (500 mg, 80% yield). HRMS analysis (APCI): calcd for $C_{42}H_{24}O_2S_2$ (M+H)$^+$, 625.1290; found, 625.1308 (error: 2.9 ppm).

Synthesis of Ph-AT-3

To a solution of triisopropylsilylacetylene (582 mg, 3.2 mmol) in anhydrous THF (30 ml) at 0 °C was added drop-wise *n*-BuLi (1.6 M in hexanes, 2.0 ml, 3.2 mmol). The solution was stirred for 30 min at 0 °C. Then quinone **6a** (208 mg, 0.5 mmol) was added as solid in one portion. The mixture was slowly warmed to room temperature and stirred overnight. Then anhydrous $SnCl_2$ (758.5 mg, 4.00 mmol) was directly added to the mixture and stirred for 12h in the dark. During this period the color of the reaction mixture became green. The resulting green solution was then filtered and the filtrate was subsequently evaporated to dryness. The residue was purified by column chromatography (silica gel, hexane/DCM, avoiding light). Compound **Ph-AT-3** was further purified by recrystallization from MeOH/CH_2Cl_2 as a dark green solid (224 mg, 60% yield).^{1}H NMR (500 MHz, $CDCl_3$, ppm): δ = 9.39 (s, 2H), 8.39-8.36 (m, 2H), 7.88 (d, *J* = 7.5 Hz, 4H), 7.54 (t, *J* = 7.7 Hz, 4H), 7.43 (t, *J* = 7.5 Hz, 2H), 7.33-7.30 (m, 2H), 1.23-1.18 (m, 42H); ^{13}C NMR (125 MHz, $CDCl_3$, ppm): δ =135.14, 134.67, 133.61, 132.86, 129.82, 129.29, 129.26, 127.60, 127.32, 126.55, 119.06, 118.61, 106.07, 104.01, 18.86, 11.51; HRMS analysis (APCI): calcd for $C_{50}H_{58}SSi_2$ (M+H)$^+$, 747.3871; found, 747.3877 (error: 0.8 ppm).

Synthesis of Ph-AT-4

To a solution of triisopropylsilylacetylene (582 mg, 3.2 mmol) in anhydrous THF (30 ml) at 0 °C was added drop-wise *n*-BuLi (1.6 M in hexanes, 2.0 ml, 3.2 mmol). The solution was stirred for 30 min at 0 °C. Then quinone **6b** (233 mg, 0.5 mmol) was added as solid in one portion. The mixture was slowly warmed to room temperature and stirred overnight. During this period the insoluble diketone disappeared and the solution became clear with strong fluorescence. Then anhydrous $SnCl_2$ (758.5 mg, 4.00 mmol) was directly added to the mixture and stirred for 12h in the dark (the RBF was strictly covered by the aluminum foil). However, thin layer chromatography indicates complicated decomposed compounds with large polarity were formed. The decomposed compounds could not be separated and identified. From MALDI-TOF mass spectrum, the oxygen adducts could be observed.

Synthesis of Ph-ADT-3-D

To a solution of triisopropylsilylacetylene (582 mg, 3.2 mmol) in anhydrous THF (30 ml) at 0 °C was added drop-wise *n*-BuLi (1.6 M in hexanes, 2.0 ml, 3.2 mmol). The solution was stirred for 30 min at 0 °C. Then quinone **7** (312 mg, 0.5 mmol) was added as solid in one portion. The mixture was slowly warmed to room temperature and stirred overnight. During this period the insoluble diketone disappeared and the solution became clear with strong fluorescence. Then anhydrous $SnCl_2$ (758.5 mg, 4.00 mmol) was directly added to the mixture and stirred for 12h in the dark (the RBF was strictly covered by the aluminum foil). During this period the color of the reaction mixture became red. The resulting red solution was then filtered and the filtrate was subsequently evaporated to dryness. The residue was purified by column chromatography (silica gel, hexane/DCM, avoiding light). Compound **Ph-ADT-3-D** was further purified by recrystallization from MeOH/CH_2Cl_2 under dark as a red solid (285 mg, 60% yield). ^{1}H NMR (500 MHz, $CDCl_3$, ppm): δ = 8.63

(s, 4H), 7.61-7.55 (m, 8H), 7.47-7.32 (m, 24H), 7.24-7.14 (m, 8H), 1.10-0.80 (m, 84H); ^{13}C NMR (125 MHz, $CDCl_3$, ppm): δ = 141.57, 137.94, 136.41, 134.80, 134.51, 133.67, 133.20, 129.86, 129.45, 129.04, 128.88, 128.80, 127.17, 127.05, 119.23, 118.38, 104.07, 103.03, 46.71, 18.90, 18.86, 11.46; HRMS analysis (ESI): calcd for $C_{128}H_{132}S_4Si_4$ $(M+H)^+$, 1909.8362; found, 1909.8339 (error: -1.2 ppm). Note: During the crystal growing of **Ph-ADT-3-D**, a trace amount of decomposed compound **Ph-ADT-3-O** was also occasionally identified by X-ray crystallographic analysis, however could not be isolated in a pure compound.

Acknowledgements

C. C. acknowledges financial support from the MOE Tier 1 grant (R-143-000-623-112) and Tier 3 programme (MOE2014-T3-1-004). We thank Dr. Bruno Donnadieu and Dr. Tan Geok Kheng for the crystallographic analysis.

Keywords: acene • non-classical acene • heteroacene • diradical character • quinoid

[1] Review articles: a) J. E. Anthony, *Chem. Rev.* **2006**, *106*, 5028-5048; b) J. E. Anthony, *Angew. Chem. Int. Ed.* **2008**, *47*, 452-483; *Angew. Chem.* **2008**, *120*, 460-492; c) Q. Ye, C. Chi, *Chem. Mater.* **2014**, *26*, 4046-4056.

[2] a) M. Bendikov, H. M. Duong, K. Starkey, K. N. Houk, E. A. Carter, F. Wudl, *J. Am. Chem. Soc.* **2004**, *126*, 7416-7417; b) C. Tönshoff, H. F. Bettinger, *Angew. Chem. Int. Ed.* **2010**, *49*, 4125-4128; *Angew. Chem.* **2010**, *122*, 4219-4222; c) R. Huang, H. Phan, T. S. Herng, P. Hu, W. Zeng, S. Dong, S. Das, Y. Shen, J. Ding, D. Casanova, J. Wu, *J. Am. Chem. Soc.* **2016**,*138*, 10323- 10330.

[3] Review articles: a) Z. Sun, Q. Ye, C. Chi, J. Wu, *Chem. Soc. Rev.* **2012**, *41*, 7857-7889; b) M. Abe, *Chem. Rev.* **2013**, *113*, 7011-7088; c) Z. Sun, Z. Zeng, J. Wu, *Acc. Chem. Res.* **2014**, *47*, 2582-2591; d) T. Kubo, *Chem. Rec.* **2015**, *15*, 218-232; e) Z. Zeng, X. Shi, C. Chi, J. T. L. Navarrete, J. Casado, J. Wu, *Chem. Soc. Rev.* **2015**, *44*, 6578-6596.

[4] a) A. Konishi, Y. Hirao, M. Nakano, A. Shimizu, E. Botek, B. Champagne, D. Shiomi, K. Sato, T. Takui, K. Matsumoto, H. Kurata, T. Kubo, *J. Am. Chem. Soc.* **2010**, *132*, 11021-11023; b) A. Konishi, Y. Hirao, K. Matsumoto, H. Kurata, R. Kishi, Y. Shigeta, M. Nakano, K. Tokunaga, K. Kamada, T. Kubo, *J. Am. Chem. Soc.* **2013**, *135*, 1430-1437; c) Z. Sun, S. Lee, K. Park, X. Zhu, W. Zhang, B. Zheng, P. Hu, Z. Zeng, S. Das, Y. Li, C. Chi, R. Li, K. Huang, J. Ding, D. Kim, J. Wu, *J. Am. Chem. Soc.* **2013**, *135*, 18229-18236.

[5] a) F. Wudl, M. Kobayashi, A. J. Heeger, *J. Org. Chem.* **1984**, *49*, 3382-3384; b) K. Nayak, D. S. Marynick, *Macromolecules* **1990**, *23*, 2237-2245; c) J. Kuerti, P. R. Surjan, M. Kertesz, *J. Am. Chem. Soc.* **1991**, *113*, 9865-9867; d) A. K. Mohanakrishnan, M. V. Lakshmikantham, M. P. Cava, R. D. Rogers, L. M. Rogers, Tetrahedron **1998**, *54*, 7075-7080.

[6] a) J. E. Anthony, S. Subramanian, S. R. Parkin, S. K. Park, T. N. Jackson, *J. Mater. Chem.* **2009**, *19*, 7984-7989; b) B. Tylleman, C. M. L. Vande Velde, J.-Y. Balandier, S. Stas, S. Sergeyev, Y. H. Geerts, *Org. Lett.* **2011**, *13*, 5208-5211; c) D. Lehnherr, A. R. Waterloo, K. P. Goetz, M. M. Payne, F. Hampel, J. E. Anthony, O. D. Jurchescu, R. R. Tykwinski, *Org. Lett.* **2012**, *14*, 3660-3663.

[7] a) M. P. Cava, G. E. M. Husbands, *J. Am. Chem. Soc.* **1969**, *91*, 3952-3953; b) M. P. Cava, N. M. Pollack, G. A. Dieterle, *J. Am. Chem. Soc.* **1973**, *95*, 2558-2560; c) M. P. Cava, M. Behforouz, G. E. M. Husbands, M. Srinivasan, *J. Am. Chem. Soc.* **1973**, *95*, 2561-2564; d) K. T. Potts, D. McKeough, *J. Am. Chem. Soc.* **1973**, *95*, 2750-2751; e) M. P. Cava, M. A. Sprecker, *J. Org. Chem.* **1973**, *38*, 3975-3978; f) M. P. Cava, M. A. Sprecker, W. R. Hall, *J. Am. Chem. Soc.* **1974**, *96*, 1817-1821; g) K. T. Potts, D. McKeough, *J. Am. Chem. Soc.* **1974**, *96*, 4268-4275; h) M. P. Cava, M. V. Lakshmikantham, *Acc. Chem. Res.* **1975**, *8*, 139-144; i) B. Djukic, D. F. Perepichka, *Chem. Commun.* **2011**, *47*, 12619-12621.

[8] a) A. L. Appleton, S. Miao, S. M. Brombosz, N. J. Berger, S. Barlow, S. R. Marder, B. M. Lawrence, K. I. Hardcastle, U. H. F. Bunz, *Org. Lett.* **2009**, *11*, 5222-5225; b) T. L. Tam, H. Li, F. Wei, K. J. Tan, C. Kloc, Y. M. Lam, S. G. Mhaisalkar, A. C. Grimsdale, *Org. Lett.* **2010**, *12*, 3340-3343.

[9] R. C. Haddon, S. R. Wasserman, F. Wudl, G. R. J. Williams, *J. Am. Chem. Soc.* **1980**, *102*, 6687-6693.

[10] D. Xia, X. Guo, L. Chen, M. Baumgarten, A. Keerthi, K. Müllen, *Angew. Chem. Int. Ed.* **2016**, *55*, 941-944; *Angew. Chem.* **2016**, *128*, 953-956.

[11] a) S. Ogawa, H. Muraoka, K. Kikuta, F. Saito, R. Sato, *J. Organomet. Chem.* **2007**, *692*, 60-69; b) J. A. Clement, A. K. Mohanakrishnan, *Tetrahedron* **2010**, *66*, 2340-2350.

[12] R. Rao M, C.-W. Liao, S.-S. Sun, *J. Mater. Chem. C* **2013**, *1*, 6386-6394.

[13] Crystallographic data of **Ph-AT-1**, **Ph-AT-2**, **Ph-AT-3**, **Ph-ADT-3-D** and **Ph-ADT-3-O** are deposed in the Cambridge Crystallographic Data Center with CCDC number of 1524007, 1524008, 1524009, 1539468, and 1524011, respectively.

[14] X. Shi, C. Chi, *Chem. Rec.* **2016**, *16*, 1690-1700.

Entry for the Table of Contents

FULL PAPER

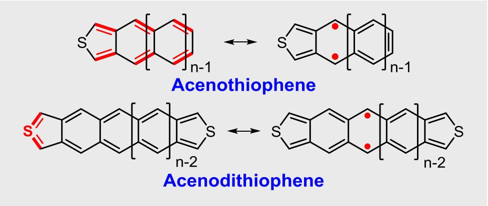

Go beyond classical acenes! Two types of non-classical *S*-heteroacenes, the acenothiophene and acenodithiophene, are investigated both theoretically and experimentally. The long non-classical *S*-heteroacenes display unusually high chemical reactivity which can be explained by their unique *o*-quinoidal conjugation as well as emerging open-shell diradical character

.

*X. Shi, T. Y. Gopalakrishna, Q. Wang, and C. Chi**

Page No. – Page No.

Non-classical *S*-Heteroacenes with *o*-Quinoidal Conjugation and Open-shell Diradical Character